

# An improved system for the automatic estimation of the Arteriolar-to-Venular diameter Ratio (AVR) in retinal images

Lara Tramontan, Enrico Grisan, *Member, IEEE*, and Alfredo Ruggeri, *Senior Member, IEEE*

**Abstract**—The Arteriolar-to-Venular diameter Ratio (AVR), a parameter derived from vessel caliber measurements in a specific region of retinal images, is used as a descriptor of generalized arteriolar narrowing, an eye fundus sign often seen in patients affected by hypertensive or diabetic retinopathies. We developed an improved system to compute AVR in a totally automatic way. Images are at first enhanced to highlight the vessel network, which is then traced by a vessel tracking algorithm. From the detected vessel structure, the position of the optic disc is derived and the region inside which the AVR data are to be measured is determined. Vessels within this region are classified as either arteries or veins, their caliber is estimated and the AVR parameter is eventually computed. Improvements with respect to the previous version are related to post-processing algorithms to enhance vessel tracking and a totally new artery/vein discrimination technique. Results provided by the new system have been compared with manually derived AVR values on 20 eye fundus images, resulting in a final correlation coefficient of 0.88.

## I. INTRODUCTION

AN early warning about serious cardiovascular diseases can be provided by the analysis of microvasculature health status. The capillary network in the retina, an important example of such microvasculature, can be readily imaged and assessed, using normal a fundus camera.

On retinal images, a sign that have been shown to be related to cardiovascular diseases is the generalized arteriolar narrowing, usually expressed by the Arteriolar-to-Venular diameter Ratio (AVR) [1]. It is computed from the values of individual arteriolar and venular calibers [2], measured in a standard area centered on the optic disc (OD) and from half-disc to one disc diameter from the OD margin. The current procedure requires the long and cumbersome manual measurement of the required vessel calibers. To overcome this problem, computer-assisted procedures have been proposed [3-4], which however still require some degree of user assistance. Our own group recently proposed an automatic system [5], evaluated on fourteen images with fairly good performances.

We propose here an improved version of that system, which is able to achieve better performances on a larger image data set, provided by one of the world leading centers for studies on hypertensive and diabetic retinopathies.

Manuscript received June 27, 2008.

Authors are with the Dept. of Information Engineering, University of Padova, 35131 Padova, Italy (corresponding author A.R. phone: +39-049-8277624; fax: +39-049-8277699; e-mail: alfredo.ruggeri@unipd.it).

## II. MATERIAL AND METHODS

Twenty color retinal images, acquired during the DCCT study [6], were made available by the Department of Ophthalmology and Visual Sciences, University of Wisconsin, USA. The 30° field of view images were saved in digital format, with a resolution of 3.7  $\mu\text{m}/\text{pixel}$ , resulting in 2346x2652 pixel images.

The fully automatic procedure to derive the AVR index requires several steps to be performed. After an initial image enhancement to improve and normalize image quality, the network of retinal vessel is traced and OD position and diameter are identified. With this information, the specific area in which caliber measurements are to be done is identified. Inside this area, vessels are labeled as either arteries or veins and their calibers are measured. Finally, caliber measurements are used to compute AVR, according to the formula proposed by Knutson et al [7].

### A. Image preprocessing

Very often retinal images are unevenly or non-uniformly illuminated and thus exhibit local luminosity and contrast variability. This problem may seriously affect any diagnostic process and its outcome, especially if an automatic computer-based procedure is used to derive the diagnostic parameters, like here.

To overcome this problem, we used a previously developed method to normalize luminosity and contrast in retinal images, both intra- and inter-image [8]. The method is based on the estimation of the luminosity and contrast variability in the background part of the image and the subsequent compensation of this variability in the whole image.

### B. Vessel Tracing

The identification and quantitative description of the vascular structure is a necessary prerequisite to compute AVR.

To this end, we employed a system we developed for the automatic extraction of the vascular structure in retinal images, which works on the green channel of the color retinal image and is based on a sparse tracking technique [9]. Starting from a set of seed points, the tracking procedure moves along the vessel (Fig. 1) by analyzing subsequent vessel cross-sections (blue segments in Fig. 1) and extracting the vessel center, caliber and direction. The pixels belonging to the vessel in a cross-section (red segments in Fig. 1) are found by means of a fuzzy C-means classifier applied to all

cross-section pixels. The center points of vessel cross-sections are called vessel sample points.

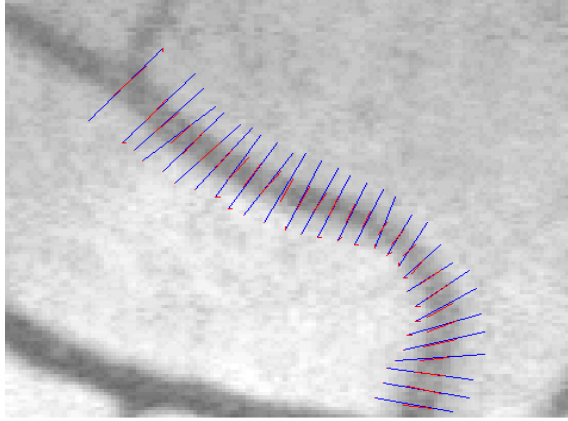


Fig. 1. Vessel tracking technique. The blue segments represent the vessel cross-sections, whereas the red segments indicate the pixels belonging to the vessel.

When tracking stops because of a critical area, e.g. low contrast, bifurcation or crossing, a “bubble technique” module is run. It is able to analyze multiple circular scan lines around the critical points, allowing the exploration of the vessel structure beyond the critical areas.

After this tracking step, identified segments are connected by a connection algorithm and bifurcations and crossings are identified by analyzing specific features of vessel end-points.

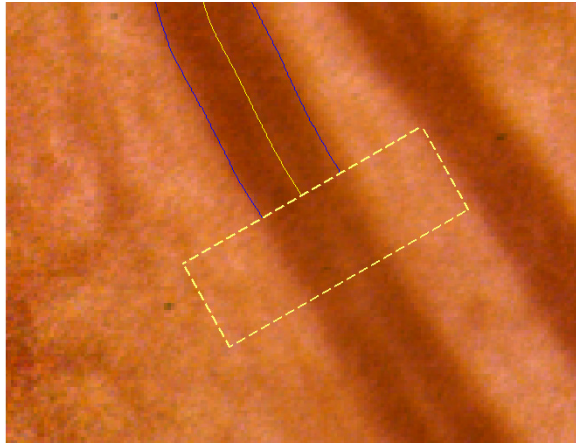


Fig. 2. The rectangular ROI (dashed yellow line) overlapping the region where vessel tracing stopped due to low vessel contrast.

### C. Tracing post-processing

The above mentioned bubble technique is not always capable of allowing the tracing module to overcome critical situations, such as areas where vessel edges are poorly contrasted with respect to background. The new post-processing technique we propose here is based on the observation that edges do not exhibit abrupt changes in direction or in distance between them. It then tries to detect vessel edges in the low contrast region using a priori information deriving from the edges previously traced. This

technique works in a rectangular ROI overlapping the critical area where vessel tracing stopped (Fig. 2).

The vessel tracing is now obtained from the process of edge detection and it is computed by applying a directional band-pass filter based on Gabor’s function  $G(x,y)$ :

$$G(x, y) = \sin(\omega x) e^{-\frac{1}{2} \left( \left( \frac{x}{\sigma_x} \right)^2 + \left( \frac{y}{\sigma_y} \right)^2 \right)} \quad (1)$$

where  $\omega$  is the central frequency and  $x$  and  $y$  are based on the ROI local coordinate frame. A threshold process is then applied to smooth discontinuities and thinning of edges by Hough transform is performed. An example of resulting edges is shown in Fig 3.

In order to better manage situations that may derive from interaction between vessels, e.g. at crossings, the standard circular area, in which AVR is computed, is partitioned into several smaller, concentric circular sub-areas, and the post-processing routine described above is applied starting from the outermost sub-area and then moving on to inner ones, gradually closing in on the OD.

In each sub-area, post-processing is run on single vessels only within the ROI length, and then iteratively applied to the other low-contrast vessels of the same sub-area.

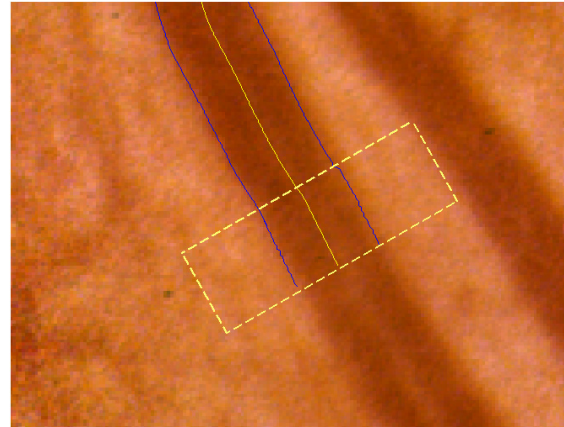


Fig. 3. The rectangular ROI of Fig. 2 with the new edges detected by applying the tracing post-processing algorithm.

### D. ROI Detection

The AVR parameter is computed from the values of individual arteriolar and venular calibers measured inside a specific region of the eye fundus, the standard area centered at the OD and from half-disc to one disc diameter from the OD margin.

To detect the OD position, we used a method previously developed [10], based on the geometrical information yielded by the network of retinal vessels. The OD diameter was assumed to be the standard value of 1850  $\mu\text{m}$  [7], and this value was also used to determine the pixel/ $\mu\text{m}$  calibration, as proposed by the Early Treatment Diabetic Retinopathy Study.

From the knowledge of OD center and diameter, the specific area for AVR computation can thus be identified on each retinal image.

### E. Artery-Vein (A/V) Discrimination

As arteriolar and venular calibers need to be separately measured to derive AVR, each traced vessel inside the ROI must be correctly labeled as either artery or vein. The algorithm we used so far [11], based on local comparison of vessel color features, was not able to perform a sufficiently correct A/V discrimination in the present image dataset. We had thus to develop a new A/V classification technique.

In these images, arteries present a clearly visible red central reflex, due to the increased reflectivity of arterial wall with respect to vein one. This observation suggested the discriminating feature to be adopted for A/V discrimination.

The red channel is extracted in each image and the pixel intensities along transversal sections of vessels (profiles), drawn across vessels with width 1.2 times the vessel caliber, are analyzed. A parameter called *red contrast*, defined as the ratio between the peak of intensity in the central part of the vessel profile and the largest value between intensities at two end-points of the profile, is evaluated (Fig. 4). Arteries show much larger values of *red contrast* than veins.

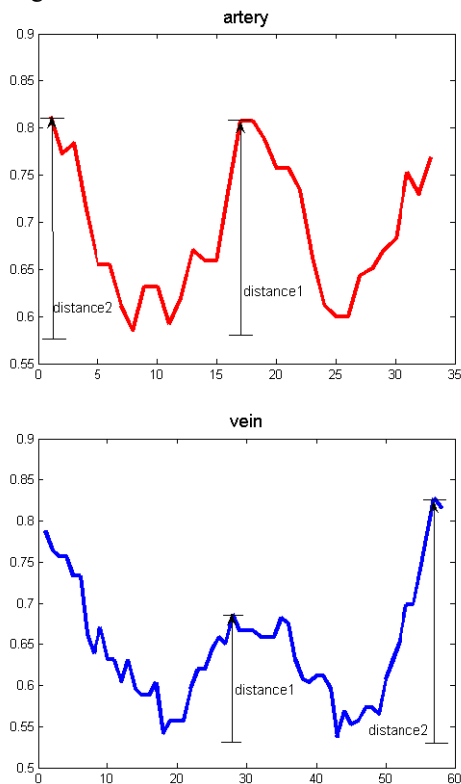


Fig. 4. The *red contrast*, given by the ratio between distance1 and distance2, shown for an artery (top) and a vein (bottom).

A probability of belonging to the vein class is thus assigned to each vessel, based on the average value of the *red contrast* along the vessel. The Hill function was chosen to describe this probability and vessels with probability higher than 0.5 are classified as veins, all other as arteries (Fig 5).

### F. AVR Estimation

From the arteriolar and venular calibers estimated as described above, the Central Retinal Artery Equivalent (CRAE) and Central Retinal Vein Equivalent (CRVE) parameters can be computed and their ratio

$$AVR = \frac{CRAE}{CRVE} \quad (1)$$

provides an indication of a possible generalized arteriolar narrowing [2,6]. AVR values smaller than 1 indicate an arteriolar diameter on average narrower than the venular one.

### G. Manual AVR Estimation

We chose to use as reference values, against which the automatic results were to be compared, the results of the manual AVR estimation performed by the experts at the Department of Ophthalmology & Visual Sciences, University of Wisconsin-Madison. This latter was carried out by manually performing all steps on the retinal images displayed on a PC monitor: identification of OD and its diameter (and thus of the ROI for caliber estimation), A/V discrimination of vessels, caliber measurement by drawing segments with the mouse and computing their pixel length.

The formulas in [7] were eventually applied to derive AVR values from the arteriolar and venular diameters.

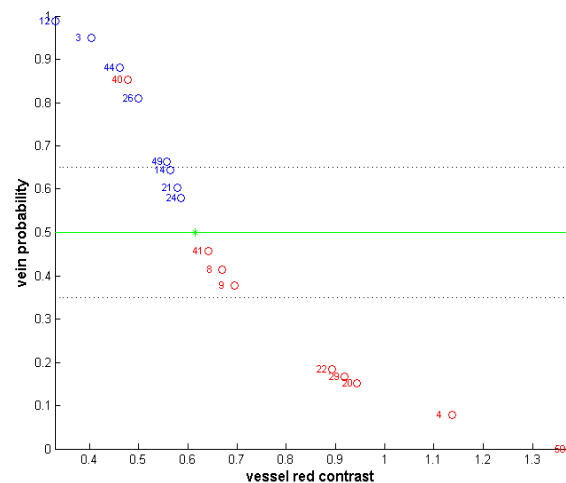


Fig. 5. Probability of being vein for vessels of one of the dataset images. True veins are in blue, true arteries in red; a classification error is present for vessel nr. 40 (red mark, upper left-hand side).

## III. RESULTS

Table I reports the manual and automatic AVR results, together with their ratios. Their scatter plot with correlation is shown in Fig. 6.

Mean and SD values from the two sets of measurements are the same, and automatic/manual ratios have an average value of 1 with a narrow 95% confidence interval (0.98-1.02). The correlation coefficient between the two methods is 0.88.

	Manual	Automatic	Aut/Man
1	0.54	0.53	<b>0.98</b>
2	0.58	0.55	<b>0.95</b>
3	0.59	0.58	<b>0.98</b>
4	0.60	0.62	<b>1.03</b>
5	0.64	0.73	<b>1.14</b>
6	0.66	0.65	<b>0.98</b>
7	0.66	0.64	<b>0.97</b>
8	0.66	0.65	<b>0.98</b>
9	0.66	0.70	<b>1.06</b>
10	0.70	0.68	<b>0.97</b>
11	0.71	0.71	<b>1.00</b>
12	0.72	0.74	<b>1.03</b>
13	0.73	0.74	<b>1.01</b>
14	0.73	0.75	<b>1.02</b>
15	0.74	0.74	<b>1.00</b>
16	0.74	0.74	<b>1.00</b>
17	0.76	0.76	<b>1.00</b>
18	0.76	0.74	<b>0.97</b>
19	0.77	0.73	<b>0.95</b>
20	0.82	0.73	<b>0.89</b>
Mean	<b>0.69</b>	<b>0.69</b>	<b>1.00</b>
SD	<b>0.07</b>	<b>0.07</b>	<b>0.05</b>
95% C.I.			<b>0.98-1.02</b>

Table I. AVR values obtained with the manual and the automatic procedure and their ratio.

#### IV. DISCUSSION AND CONCLUSIONS

The AVR values estimated by the automatic procedure are quite close to the ones provided by the manual one.

In only two images (nr. 5 and nr. 20), the ratio between measurements is appreciably different from unity, with values of 1.14 and 0.89 respectively. A detailed analysis of these cases revealed that in each image the wrong classification of one vessel only was the cause for these unsatisfactory results. When these misclassifications are manually corrected, e.g. with a quick editing tool that can be easily made available to the user, the ratios become 0.95 and 0.99, respectively, and the overall correlation coefficient becomes 0.97. Work is however in progress to refine the A/V discrimination technique, e.g. by combining additional vessel features in the vein probability function.

Additional evaluations on larger set of images, acquired from subjects exhibiting much wider variations of AVR, will be performed in order to fully assess the reliability and clinical applicability of this automatic procedure.

#### ACKNOWLEDGMENT

The authors wish to thank L. Hubbard and colleagues, from the Department of Ophthalmology and Visual Sciences, University of Wisconsin, Madison, WI (USA), for providing retinal images and reference AVR data.

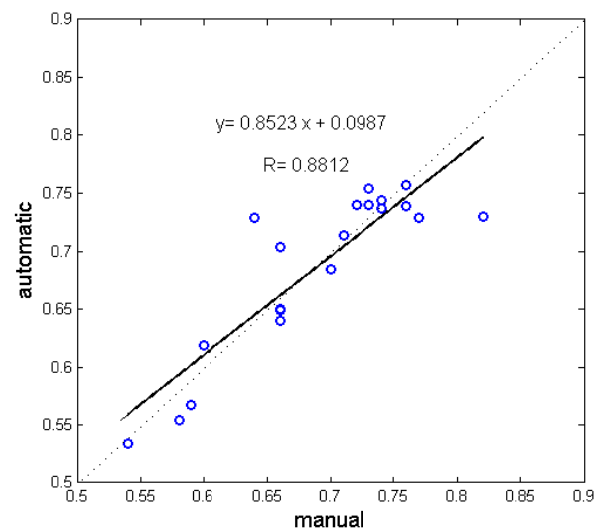


Fig. 6. Scatter plot of AVR values from the manual and the automatic procedure. The solid line indicates the regression line and the dashed line is the identity line.

#### REFERENCES

- [1] T. Y. Wong, R. Klein, B. E. K. Klein, and J. M. Tielsch et al., "Retinal microvascular abnormalities, and their relation to hypertension, cardiovascular diseases and mortality," *Survey Ophthalmol.*, vol. 46, pp. 59–80, 2001.
- [2] L. D. Hubbard and R. J. Brothers et al., "Methods for evaluation of retinal microvascular abnormalities associated with hypertension/sclerosis in the atherosclerosis risk in communities studies," *Ophthalmology*, vol. 106, pp. 2269–80, 1999.
- [3] T. Y. Wong, M. Knudtson, R. Klein, B. E. K. Klein, S.M. Meuer, L. D. Hubbard, "Computer-assisted measurement of retinal vessel diameters in the Beaver Dam eye study," *Ophthalmology*, vol. 111, pp. 1183–90, 2004.
- [4] H. Li, W. Hsu, M.L. Lee, and T.Y. Wong "Automatic grading of retinal vessel caliber," *IEEE Trans Biomed Eng*, vol. 52, pp. 1352–5, 2005.
- [5] A. Ruggeri, E. Grisan, M. De Luca "An automatic system for the estimation of generalized arteriolar narrowing in retinal images," *Proc. 29th Annual International Conference of IEEE-EMBS*, pp. 6463–6, IEEE, New York, 2007.
- [6] The DCCT Research Group "Color photography vs. fluorescein angiography in the detection of diabetic retinopathy in the Diabetes Control and Complications Trial," *Arch Ophthalmol*, vol. 105, pp. 1344–51, 1987.
- [7] M.D. Knudtson, K.E. Lee, L.H. Hubbard, T.Y. Wong, R. Klein, B.E.K. Klein, "Revised formulas for summarizing retinal vessel diameters," *Current Eye Research*, vol. 27, no. 3, pp. 143–149, 2003.
- [8] M. Foracchia, E. Grisan and A. Ruggeri, "Luminosity and contrast normalization in retinal images," *Med Image Anal*, vol. 9, pp. 179–90, 2005.
- [9] E. Grisan, A. Pesce, A. Giani, M. Foracchia, and A. Ruggeri, "A new tracking system for the robust extraction of retinal vessel structure," *Proc. 26th Annual International Conference of IEEE-EMBS*, pp. 1620–3, IEEE, New York, 2004.
- [10] M. Foracchia, E. Grisan and A. Ruggeri, "Detection of optic disc in retinal images by means of a geometrical model of vessel structure," *IEEE Trans Med Imag*, vol. 23, pp. 1189–95, Oct 2004.
- [11] E. Grisan and A. Ruggeri, "A divide et impera strategy for automatic classification of retinal vessels into arteries and veins," *Proc. 25th Annual International Conference of IEEE-EMBS*, pp. 890–4, IEEE, New York, 2003.